Friction law and hysteresis in granular materials

E. DeGiuli and M. Wyart
Institute of Physics, Ecole Polytechnique Fédérale de Lausanne (EPFL), CH-1015 Lausanne, Switzerland

The macroscopic friction of particulate materials often weakens as the flow rate is increased, leading to potentially disastrous intermittent phenomena including earthquakes and landslides. We theoretically and numerically study this phenomenon in simple granular materials. We show that velocity-weakening, corresponding to a non-monotonic behavior in the friction law $\mu(I)$, is present even if the dynamic and static microscopic friction coefficients are identical, but disappears for softer particles. We argue that this instability is induced by endogenous acoustic noise, which tends to make contacts slide, leading to faster flow and increased noise. We show that soft spots, or excitable regions in the materials, correspond to rolling contacts that are about to slide, whose density is described by a nontrivial exponent θ_s. We build a microscopic theory for the non-monotonicity of $\mu(I)$, which also predicts the scaling behavior of acoustic noise, the fraction of sliding contacts χ and the sliding velocity, in terms of θ_s. Surprisingly, these quantities have no limit when particles become infinitely hard, as confirmed numerically. Our analysis rationalizes previously unexplained observations and makes new experimentally testable predictions.

arXiv:1704.00740v1 [cond-mat.soft] 3 Apr 2017

A central property of particulate materials is their macroscopic friction [1, 2]. In velocity-strengthening materials, friction grows with the deformation rate and flow is stable. By contrast, velocity-weakening materials are susceptible to instabilities under loading, including stick-slip. This classification is believed to distinguish faults that are prone or not to earthquakes [3], which ultimately corresponds to the shear of a granular material made of rocks and debris – the gouge – contained within the narrow fault between two tectonic plates. The Rice-Ruina rate-and-state model can describe both kinds of frictional behavior [4]. It is, however, a heuristic model, and building a microscopic theory to justify *a priori* which materials weaken or strengthen under flow remains a challenge. To make progress, it is natural to consider well-controlled granular materials such as glass beads or sand, which have received considerable attention in the last decades. In these systems an important result comes from dimensional analysis: assuming that grains are strictly hard and that this limit is not singular, the macroscopic friction or stress ratio $\mu \equiv \sigma/p$, where σ is shear stress and p is pressure, can be shown to depend on strain rate $\dot{\epsilon}$ and pressure only via the dimensionless inertial number $I \equiv \dot{\epsilon} D\sqrt{\rho/p}$. Here D is mean grain diameter and ρ is grain density [5–7]. The constitutive relation $\mu(I)$ has been extensively studied in the range $I \geq 10^{-3}$ and is found to be a growing function of I, corresponding to a velocity-strengthening material. However, several recent experiments have reported non-monotonic behavior of $\mu(I)$ for very small I[8–10], corresponding to velocity weakening. There is currently no microscopic theory rationalizing these observations.

As depicted in Fig.1a, the non-monotonic behavior of $\mu(I)$ must lead to hysteresis effects, that are well-known to characterize the jamming transition of granular materials. Indeed, the maximum angle of repose of a granular layer θ_{start} (corresponding to a macroscopic friction $\mu_{start} = \tan(\theta_{start})$) is larger than the angle θ_{stop} where avalanches stop (corresponding to $\mu_{stop} = \tan(\theta_{stop})$) [11]. Several properties of this hysteresis should be explained by a microscopic theory: (i) externally applied vibrations [8, 10, 12, 13] can eliminate hysteresis, if the vibration velocity passes a threshold amplitude [13]. (ii) Hysteresis appears to become very small if inertial effects are negligible [14]. (iii) There is no evidence of hysteresis for frictionless particles [15] [16].

In this letter we build a microscopic theory that explains these observations, and justify why for hard enough frictional particles $\mu(I)$ is non-monotonic at small inertial numbers. Our results, which we test using the discrete element method, hold even if the friction between two particles is assumed to be a simple Coulomb law with identical static and dynamic friction coefficients. This demonstrates that hysteresis emerges as a collective effect, even when absent at the contact level. Our approach is based on two previous fundamental insights. First, acoustic emissions generated by particle collisions during flow can fluidize the granular material, reducing dissipation. This idea was proposed by Melosh [17–19] to explain why the macroscopic friction μ can be reduced by a factor of order 10 from its static value during earthquakes. However, the quantitative treatment of this effect has been criticized [20], and the role of self-fluidization in regular granular materials is unclear.

To quantify this role, we will use a second, recent insight: elementary excitations are a key feature of amorphous solids, in particular their density affects the material stability and its susceptibility to flow plastically [21–23]. These excitations correspond to soft spots – equivalent to dislocations in metals – where local rearrangements can be triggered if the stress is increased, or if mechanical noise is present. For hard frictionless particles, excitations correspond to contacts carrying a small force, which are thus susceptible to open [21, 24, 25]. Here we will argue that for frictional granular materials, another kind of excitation appears, associated with contacts that are very close to sliding. Denoting by δf the distance to sliding of a contact, we find that the distribution of excitations follows $P(\delta f) \sim \delta f^{\theta_s}$ with $\theta_s \approx -1/3$. From this knowledge, we can compute the effect of mechanical

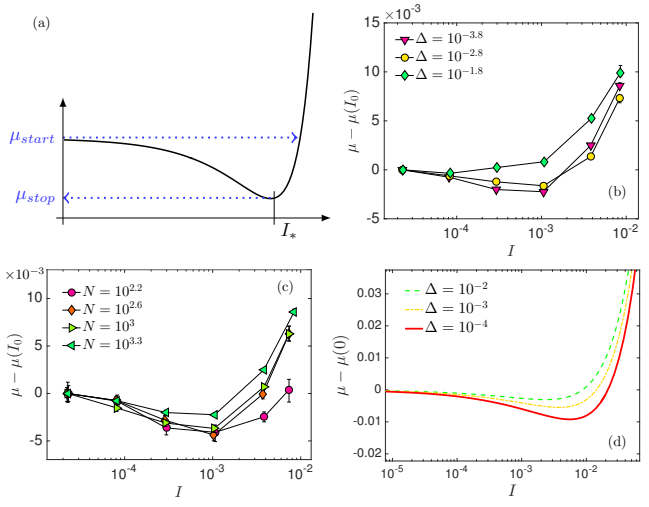

FIG. 1: (a) Sketch illustrating that non-monotonic macroscopic friction leads to hysteresis. In a stress ramp from $\mu = 0$, flow will begin at μ_{start}, while in a stress decrease from large I, flow will stop at μ_{stop} and a finite I. (b,c) Numerical results for $\mu(I, \Delta) - \mu(I_0, \Delta)$ confirm the existence of a non-monotonic curve. In (b), $N = 10^{3.3}$ and Δ is varied, while in (c) $\Delta \approx 10^{-4}$ and N is varied. $I_0 = 2 \times 10^{-5}$ is the smallest simulated I. (d) The qualitative behavior of $\mu(I, \Delta)$ is reproduced by a phenomenological model (Eq. 2).

noise on the structure, which in turn affects the noise itself. Ultimately this leads to an experimentally testable microscopic theory of velocity weakening and mechanical noise. In addition, several non-trivial exponents are predicted that characterize noise and other microscopic quantities, which we find to be in good agreement with our numerical results.

I. NUMERICAL EVIDENCE FOR NON-MONOTONIC FLOW CURVES

The macroscopic friction $\mu(I)$ has been studied extensively for inertial numbers $I \geq 10^{-3}$ [5–7, 26]. In the range $0.1 \geq I \geq 10^{-3}$ it follows

$$\mu(I) \approx \mu_c + c_1 I^{\alpha_\mu}. \quad (1)$$

This velocity-strengthening behavior is caused by an increase in the dissipation induced by collisions as I increases [27, 28]. There is, however, no microscopic theory for the value of α_μ, except for frictionless particles [21]. For frictional particles one observes $\alpha_\mu \approx 0.85$ [29], often approximated as $\alpha_\mu = 1$.

Here we seek to numerically study if $\mu(I)$ becomes non-monotonic in the quasi-static regime $I \leq 10^{-3}$. However, if velocity-weakening is indeed present, then homogeneous flow is unstable, and shear bands or chaotic behavior are expected. Experimental reports of velocity-weakening use a set-up with stress gradients [8–10], which has been argued to stabilize flow, but makes quantitative analysis challenging. Here instead we use the fact that shear bands have a minimal thickness (typically of order ten grain diameters wide), and that flow can be stabilized by considering small systems. Then, if μ has an instability, the non-monotonicity will be most pronounced for small N, and decay as larger systems are considered.

In practice, our numerical results are created with the standard Discrete Element Method. We work in spatial dimension $d = 2$ (our theoretical conclusions do not depend on d). The frictional disks follow static Coulomb friction: at each contact, the transverse component f_T and normal component f_N must satisfy $|f_T| \leq \mu_p f_N$, where we take the Coulomb friction coefficient to be $\mu_p = 0.3$. This coefficient is the same for static and dynamic motion. Systems are simply sheared by horizontal motion of walls at the top and bottom domain edges, on a periodic domain. The confining pressure is controlled by fixed vertical forces exerted upon the walls. Particles have linear elastic-dashpot interactions, modeling a finite restitution coefficient $e < 1$ and a particle stiffness k. $\Delta = p/k$, which characterizes the typical contact deflection relative to the grain diameter, is varied from $\Delta \approx 10^{-2}$ to $\Delta \approx 10^{-5}$.

Our results for $\mu(I)$ are shown in Figs. 1b,1c. A crucial finding is that non-monotonicity is indeed observed, but disappears if particles are too deformed (large Δ). For $\Delta \approx 10^{-4}, 10^{-3}$ we find that the minimum occurs at $I_* \approx 10^{-3}$, the same inertial number below which intermittency and large fluctuations were previously observed in simulations [6]. We measure the amplitude of non-monotonicity as $\Delta\mu_{hyst} \equiv \mu(I_0) - \mu(I_*)$ where $I_0 = 2 \times 10^{-5}$ is the smallest inertial number we probe. As expected, $\Delta\mu_{hyst}$ increases as smaller systems are considered, but I_* does not vary significantly, as shown in Fig.1c and in SI. The existence of a minimum at any finite I_* implies a dramatic behaviour as the shear stress is increased from the solid phase, as illustrated in Fig. 1a, in particular flow is predicted to start at a finite inertial number $I \approx 2 \times 10^{-3}$. Essential questions include what microscopic mechanism leads to a minimum of $\mu(I)$ at I_*, and why does this instability disappear when Δ increases?

II. MECHANISM FOR INSTABILITY IN GRANULAR MEDIA

We argue that these questions are naturally explained if one considers the role of the acoustic noise endogenously generated in flow. In dense flows of hard particles, a network of contacts is formed that constrains motion: particles cannot overlap and cannot slide if the considered contact satisfies the Coulomb criterion. For infinitely hard particles, the dynamics only occurs along floppy modes for which these constraints are satisfied [30]. For any finite Δ, there will exist small-amplitude motion orthogonal to the floppy modes, which corresponds

to vibrations of the contact network. The formation of new contacts – collisions – pumps energy into these vibrations, which eventually decays due to grain viscoelasticity. Henceforth we call this vibrational energy per particle "mechanical noise" and denote it E_{noise}. If this noise is not negligible with respect to the characteristic potential energy in the contact, $E_p \propto \Delta^2$, it will affect the contact network and "lubricate" it. In turn, this lubrication will facilitate particle motion, leading to faster flow, stronger collisions and larger noise. Our contention is that this positive feedback is responsible for instability in the flow curve and its associated hysteresis. This view naturally explains (i) why increasing particle deformability diminishes hysteresis, since it increases the potential energy which makes contacts less sensitive to noise, (ii) why immersing the grains in a viscous fluid reduces hysteresis, since it damps vibrations faster and (iii) why externally applied vibrations can eliminate hysteresis, since if the external noise is much larger than the endogenous noise, the positive feedback becomes negligible.

We now argue more specifically that the dominant "lubricating" effect of mechanical noise is to intermittently remove rolling constraints, thus increasing the fraction of sliding contacts χ. It is important to note that, with respect to noise, rolling constraints and no-overlap constraints are qualitatively different. Noise can lead to fluctuations in the distance between two particles in contact, but will never allow them to eventually penetrate each other. By contrast, vibration leading to intermittent stick-slip motion at a contact yields net relative motion between particles. This is illustrated by an object sitting on an inclined plane, which will eventually slide down if the plane is vibrated sufficiently. In our approach, this distinction explains why frictionless particles do not appear to present noticeable hysteresis [15]. (For highly deformable particles, other mechanisms than the removal of constraints described here could lead to a finite amount of hysteresis [31]).

If χ is indeed controlled by mechanical noise, then it should be a function of *both* I and Δ. This prediction is confirmed in Fig. 2, which shows that χ is a function of $I/\Delta^{1/4}$. Intriguingly, this result implies that the hard sphere limit $\Delta \to 0$ is singular, at least for some microscopic properties. In the next section we will build a quantitative theory of mechanical noise and explain this scaling property. First, we argue why this behavior of χ can indeed generate hysteresis.

Consider the following Gedankenexperiment: the stress is increased in a granular solid. According to Eq.1, flow will start when μ reaches μ_c. Now, consider the same protocol, but with vibrations imposed on the sample. Because of this noise, some contacts that were close to the Coulomb cone, as pictured in Fig.3a, will intermittently slide, leading to an overall increase of the fraction of sliding contacts, χ. Being less constrained, the material will be less stable and start flowing earlier, for some $\tilde{\mu_c} < \mu_c$. We write $\tilde{\mu}_c = \mu_c g(\chi)$, where g is a decreasing function and $g(0) = 1$. The same reduction of macroscopic static

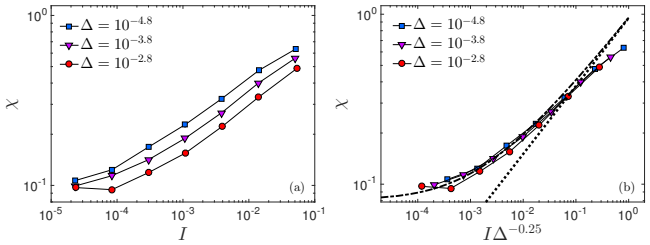

FIG. 2: (a) The density of sliding contacts, χ, depends both on I and Δ. (b) This dependence can be collapsed by plotting χ vs $I/\Delta^{1/4}$. The dotted line shows Eq.5. If finite size effects are taken into account ($\chi_c > 0$), theory predicts the dash-dotted line (SI). Here $N = 10^3$.

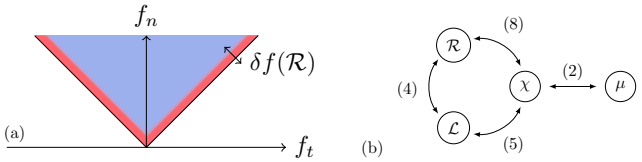

FIG. 3: (a) Sketch of Coulomb cone. Mechanical noise of magnitude $\mathcal{R}$ induces force fluctuations of a size $\delta f(\mathcal{R})$. Contacts within this distance of the edge of the Coulomb cone may be induced to slide by noise. (b) Schematic of logical relationships in theory between stress ratio μ, density of sliding contacts χ, dimensionless mechanical noise amplitude, $\mathcal{R}$, and dimensionless velocity scale, $\mathcal{L}$. Numbers denote relevant equations.

friction must apply when noise is endogenously generated in flow. This effect can be included in Eq.1, which now becomes (taking $\alpha_\mu = 1$ for simplicity):

$$\mu(I) \approx \tilde{\mu}_c + c_1 I = \mu_c + \mu_c(g(\chi) - 1) + c_1 I. \qquad (2)$$

In this equation the last term is the usual velocity-strengthening effect due to the increased dissipation induced by collisions. The second-to-last term instead is velocity-weakening. To illustrate this point we consider a linear model $g(\chi) = 1 - b\chi$. Qualitative results do not depend on the parameter b; here we choose $b = 0.3$. Other parameters entering Eq.2 are fixed by previous observations to $c_1 \approx 1.4, \mu_c \approx 0.2$. Using fits to χ from Fig.2 (described in SI), Eq.2 predicts the curves shown in Fig. 1d. We see that the qualitative features of $\mu(I)$ are captured: μ has a minimum, whose depth, but not its location, depends strongly on Δ.

III. MICROSCOPIC DESCRIPTION OF MECHANICAL NOISE

Our approach to compute the mechanical noise and its effect on χ is illustrated in Fig. 3b. We proceed in three steps. First, we express the mechanical noise in terms of

two kinetic properties: the dimensionless velocity fluctuations $\mathcal{L} = V_r/(\dot{\epsilon}D)$ (where V_r is the typical relative velocity between neighboring particles, D the particle size and $\dot{\epsilon}$ the strain rate) and ϵ_v, the characteristic strain at which particles collide and change direction. Second, we use a previous argument based on energy balance relating χ to the normalized typical sliding velocity $\mathcal{L}_T$. Finally, we compute the density of sliding contacts χ induced by the mechanical noise. This requires knowing the density of rolling contacts that are at a small distance δf to sliding. From these three coupled equations quantities of interests are derived.

Along the way we make two approximations. First, we assume that the characteristic velocity $\mathcal{L}$ with which particles collide is identical to the characteristic sliding velocity $\mathcal{L}_T$. Assuming that there is only a single velocity scale in flow is essentially a mean-field approximation, known to be correct for frictionless particles [21] but not exact for frictional ones [28]. Second, we assume that the vibrational noise is damped at a rate $1/\tau$, independently from the distance to jamming, which allows us to estimate the scaling of E_{noise} directly in terms of the energy dissipated in collisions. The usefulness of these approximations is supported by the good comparison between predictions and numerics.

Computing mechanical noise from kinetics – E_{noise} characterizes the density of vibrational energy of the contact network. The power injected in vibrational modes is supplied by collisions at a rate $\mathcal{D}_{coll}$. It can be estimated as the product of the kinetic energy of a particle $\sim \mathcal{L}^2\dot{\epsilon}^2 mD^2$ times the collisional rate $\sim \dot{\epsilon}/\epsilon_v$, leading to $\mathcal{D}_{coll} \sim \mathcal{L}^2\dot{\epsilon}^3 mD^2/\epsilon_v$ [21, 28]. Introducing a time scale τ at which this vibrational energy is dissipated into heat, we get the estimate $E_{noise} = \tau\mathcal{D}_{coll}$. We make the simplifying assumption that τ does not depend on I, characterizing the distance to jamming. Then dimensional analysis implies that $\tau = C_0 m/\eta_N$ where η_N the damping coefficient of the particle interaction. In our approximation C_0 is a constant, which we expect to be rather large [31]. Normalizing E_{noise} by the typical potential energy in a contact $E_p = \frac{1}{2}k\Delta^2 D^2$, we define their ratio

$$\mathcal{R} \equiv \frac{E_{noise}}{E_p} \propto \frac{\mathcal{D}_{coll}}{\Delta^2}\frac{\tau}{kD^2}. \tag{3}$$

Neglecting pre-factors, we obtain the scaling behavior:

$$\mathcal{R} \sim Q\frac{\mathcal{L}^2 I^3}{\Delta^{1/2}\epsilon_v} \sim Q\mathcal{L}^2\left(\frac{I}{\Delta^{1/4}}\right)^2, \tag{4}$$

where $Q \equiv \sqrt{mk/\eta_N^2}$ is the bare quality factor of the grains. We used the definition $I \equiv \dot{\epsilon}D\sqrt{\rho/p}$ as well as the previous result $\epsilon_v \propto I$ observed experimentally [32], numerically [21, 28, 33] and justified theoretically in [21, 28].

Constraint from energy balance – For realistic microscopic friction coefficient, it is found in dense flows that most of the dissipation is induced by sliding at frictional contacts [28] (the collisional dissipation $\mathcal{D}_{coll}$ is sub-dominant, but is the only one contributing to the mechanical noise). On average, the power dissipated in steady flow must balance the power injected by the shear stress; by a straightforward estimation of the sliding dissipation rate in terms of the typical sliding velocity [28], this implies that [16]:

$$\mathcal{L}_T \propto 1/\chi. \tag{5}$$

where $\mathcal{L}_T$ is the characteristic dimensionless sliding velocity of sliding contacts. In what follows we assume $\mathcal{L}_T \sim \mathcal{L}$, which is an approximation [28, 34].

Noise-induced sliding – For harmonic grains, the mechanical noise corresponds to a characteristic force scale

$$\delta\tilde{f} = pD^{d-1}\mathcal{R}^{1/2}. \tag{6}$$

$\delta\tilde{f}$ characterizes the fluctuations of forces at contacts. Such fluctuations will induce contacts *near* the edge of the Coulomb cone, shown in red in Fig.3, to slide intermittently. Thus, it is of crucial importance to determine the effect of noise on the density of contacts at small distances $\tilde{x} = f_N - |f_T|/\mu_p$ from the Coulomb cone. Fig.4 shows the distribution $P(x)$ of the dimensionless quantity $x = \tilde{x}/pD^{d-1}$. As I decreases, $P(x)$ develops a divergence $P(x) \sim x^{\theta_s}$ where $\theta_s \approx -1/3$. At any time, we expect that about half of the contacts within a dimensionless distance $\delta f = \delta\tilde{f}/pD^{d-1}$ of the Coulomb cone will be induced to slide, implying

$$\chi - \chi_c \approx \frac{1}{2}\int_0^{\delta f} dx P(x), \tag{7}$$

where χ_c corresponds to the density of sliding contacts in the system when flow stops and noise is absent. As shown in SI, our numerics support that $\chi_c \to 0$ in the thermodynamic limit, but is finite for finite N. In what follows we therefore consider $\chi_c = 0$, but our theory can readily be extended to the case $\chi_c > 0$ to capture some finite size effects, see S.I. Inserting the scaling behavior $P(x) \sim x^{\theta_s}$ in Eq.7 leads to

$$\chi \propto \tfrac{1}{2}\mathcal{R}^{\frac{1+\theta_s}{2}}. \tag{8}$$

Results – Combining Eqs.4,5,8 and keeping only on the dependence on I and Δ leads to[35]:

$$\chi \sim (I/\Delta^{1/4})^{\alpha}, \tag{9}$$

$$\mathcal{L}_T \sim (I/\Delta^{1/4})^{-\alpha}, \tag{10}$$

$$\mathcal{R} \sim (I/\Delta^{1/4})^{\gamma}, \tag{11}$$

$$\delta f \sim (I/\Delta^{1/4})^{\beta} \tag{12}$$

where $\alpha = \frac{1+\theta_s}{2+\theta_s} \approx 2/5$, $\gamma = \frac{2}{2+\theta_s} \approx 1.2$ and $\beta = \frac{1}{2+\theta_s} \approx 0.6$. In Eq.12 the characteristic dimensionless fluctuation of forces is obtained from Eq.6, and follows $\delta f \sim \mathcal{R}^{1/2}$.

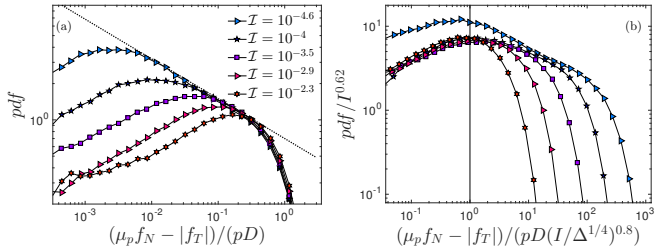

FIG. 4: Probability density function (pdf) of distance to the edge of the Coulomb cone, rescaled by p, at I indicated in (b), for $\Delta \approx 10^{-5}$. (a) raw data, and (b) rescaled with $(I/\Delta^{1/4})^{0.8}$. The dashed line shows a slope $-1/3$.

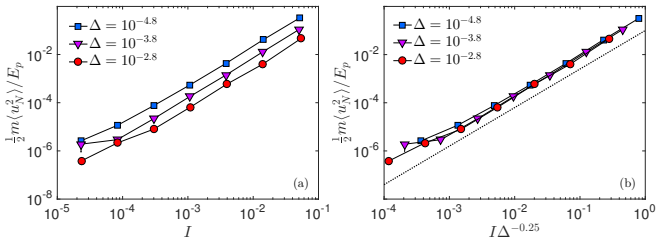

FIG. 5: Ratio of estimated energy of mechanical noise $\frac{1}{2}m\langle u_N^2\rangle$ to the potential energy scale $\frac{1}{2}k\Delta^2D^2$. This is an approximation for $\mathcal{R}$ defined as in Eq.3, shown (a) vs I, and (b) vs $I/\Delta^{1/4}$. The dotted line in (b) has a slope 1.6.

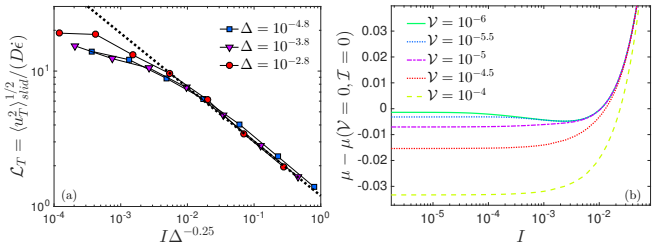

FIG. 6: (a) The sliding velocity at contacts collapses when plotted vs $I/\Delta^{1/4}$; dotted line shows $(I/\Delta^{1/4})^{-2/5}$, predicted by theory. (b) Effect of external vibrations on rheology, for various dimensionless amplitude of external noise, $\mathcal{V}$, as predicted by the phenomenological model.

These fluctuations are expected to smoothen the distribution of the distance to the Coulomb cone $P(x)$ for $x \ll \delta f$. δf can thus be extracted numerically by locating where the power law $P(x) \sim x^{\theta_s}$ breaks down, as shown in Fig.4b.

Eq.9 is tested in Fig.2, Eq.11 in Fig.5, Eq.12 in Fig.4 and Eq.10 in Fig.6. Note that testing Eq.11 requires measurement of E_{noise}, which is difficult to do directly in the numerics, as it would require identification of all the vibrational modes of the contact network, at all instants of time. To test Eq.11 we measure a proxy for E_{noise}: the characteristic kinetic energy in the relative motion between particles $m\langle u_N^2\rangle/2$, where u_N is the normal velocity at contact, as shown in Fig.5. It is a lower-bound on E_{noise} [31].

Our prediction that the correct scaling variable for these macroscopic quantities is $I/\Delta^{1/4}$ is in perfect agreement with data. The predicted exponent α of Eq.10 is in excellent agreement with observations. This is also true for Eq.9 if finite size effects are included in the theory (see SI). Our measurements for the other exponents give $\gamma = 1.6$ (Fig.5b) and $\beta = 0.8$ (Fig.6b), overall in good agreement with predictions, considering the approximations made.

These results correspond to a detailed microscopic description of mechanical noise in granular materials. It is mean-field in character, but already appears to capture the essential aspects of the phenomenon. Obviously, the contact mechanics of real granular media can be much more complicated than the harmonic contact description discussed here [4, 36]. For example, real grains in three dimensions are Hertzian, with an elastic potential $V(h) \propto E(h/D)^{5/2}$, where E is the grain Young's modulus. For such grains, the typical dimensionless contact deflection $\Delta \propto (p/E)^{2/3}$ and the characteristic stiffness scales as $k \propto ED(p/E)^{1/6}$ [37]. This entails that $\delta f \propto E_{noise}^{3/5}$. Likewise, the damping coefficient η_N may also depend on Δ. Our framework can readily be extended to include these different contact properties, which can slightly alter scaling exponents, but will not change the physical picture.

Another important possibility to consider is that the dynamic friction coefficient is smaller than the static one. This will not affect the description of mechanical noise leading to Eqs.9,10,11,12. However, it will cause the macroscopic friction to decrease even more with the fraction of sliding contacts χ. In our phenomenological model, it corresponds to an increase in the coefficient b appearing in Eq.2, which will enhance the amplitude of hysteresis.

IV. EXTERNAL NOISE IN GRANULAR FLOWS

Applying external vibrations is known experimentally to affect rheological properties and hysteresis [8, 10, 13, 36, 38, 39], as we now quantify. Even small typical noise can generate very rare events where noise is locally large, leading to rearrangements and creep flow. We do not seek to describe this effect here, which occurs at very small inertial number [10]. Instead we focus on the dynamical range relevant to hysteresis and to our theory. When a sheared material is subject to external noise, the dimensionless noise $\mathcal{R}$ will get an additional contribution. Let E_e be the characteristic energy per grain from the external noise, and define $\mathcal{R}_{ext} \equiv E_e/E_p \sim (\mathcal{V}/\Delta)^2$, where $\mathcal{V} = \sqrt{E_e/(\frac{1}{2}kD^2)}$ and $\mathcal{R}_{tot} = \mathcal{R} + \mathcal{R}_{ext}$. Using

Eqs.4,5 for $\mathcal{R}$, and Eq.8 with $\mathcal{R}_{tot}$ in place of $\mathcal{R}$, we find

$$\mathcal{R}_{tot} \sim Q\mathcal{R}_{tot}^{-1-\theta_s}\left(\frac{I}{\Delta^{1/4}}\right)^2 + \frac{\mathcal{V}^2}{\Delta^2}. \qquad (13)$$

Thus external noise is relevant for $I \lesssim I^\dagger$, where $I^\dagger \sim \mathcal{V}^{2+\theta_s}\,\Delta^{-7/4-\theta_s}\,Q^{-1/2}$. The results of Eq.13 are shown in Fig. 6b for a range of $\mathcal{V}$ (with $\theta_s = -1/3$). There are two regimes: for weak noise, μ remains non-monotonic, but the value of μ_c is lowered. However, as noise is increased and $I^\dagger > I_*$, the non-monotonicity of μ disappears entirely. We thus predict that for sufficiently strong applied noise, flow becomes stable and hysteresis disappears.

In the slider-block experiments of [13], a block is pulled over a granular bed in the presence of external vibrations of amplitude A and frequency ω. A transition from stick-slip to steady motion is observed, which does not depend on A and ω independently, but only on their product $A\omega$. This is expected from our analysis, since the external vibrational noise controlling the transition should be of order $E_e \sim \frac{1}{2}m(A\omega)^2$, indeed a function of $A\omega$ only.

Our framework can also predict the noise needed to trigger flow in a static granular material whose stress ratio is $\mu = \mu_c - \delta\mu$. Yielding will occur when the noise-induced reduction of static macroscopic friction is larger than $\delta\mu$, which according to Eqs.2,8 occurs when $\delta\mu < b\mu_c\chi \sim b\mu_c\big(\mathcal{V}/\Delta\big)^{1+\theta_s}$ or

$$\mathcal{V} > C\Delta(\delta\mu)^{1/(1+\theta_s)}, \qquad (14)$$

where C is a constant. This prediction is consistent with the earlier observation that the noise threshold increases with the confining pressure [40, 41]. It would be interesting to test further the dependence of this threshold on $\delta\mu$.

V. CONCLUSION & OUTLOOK

We have shown that velocity-weakening in dry granular flows is a collective phenomenon, which emerges even if absent at the contact level. We have explained this observation based on a microscopic theory characterizing the endogenous mechanical noise induced by collisions, as well as its effect on the structure. To understand the latter a characterization of elementary excitations on granular packings was performed, argued here to correspond to contacts that are rolling, but close to sliding. This framework rationalizes several experimental observations, including the factors governing the strength of hysteresis and the effects of exogenous noise. It also makes detailed scaling predictions on the noise level, the fraction of sliding contacts and the typical sliding velocity, in good agreement with numerical observations. Several new predictions are made that can be experimentally tested, most obviously the fact that velocity weakening should become very small or even vanish if sufficiently deformable particles are considered. This could be checked in an inclined plane experiment. From a theoretical perspective, an important question for the future is what determines the exponent θ_s characterizing excitations in frictional packings – a question now well-understood for hard frictionless particles [24, 42].

It is interesting to compare our results to Melosh's work on earthquakes [17, 18], where he proposed that acoustic emission fluidizes the fault gouge and causes the macroscopic friction to drop by a factor of order ten, as observed [43]. Melosh assumes that most of the energy dissipated goes into vibrations, whereas we find numerically in granular flows that for inertial numbers of interest for velocity weakening (say $I = 10^{-3}$), this is only true for a few percent of the injected power [28]. Likewise, in granular materials the hysteresis is a small effect, 10% at most [1]. Why such effects would be much larger in the context of a fault gouge is currently unclear, although it has been reported based on landslides that velocity weakening effects appear to grow with the length scale of the phenomenon considered [19].

Finally, it would be desirable to extend the present description to over-damped non-Brownian dense suspensions. Earlier experiments show that hysteresis increases with inertia, but do not rule out a finite amount of hysteresis in the viscous limit [14, 44]. Over-damped simulations support that the density of sliding contacts χ increases with the viscous number [34] (playing a role similar to the inertial number), but very weakly. Following the discussion of Eq.2, this behavior may be sufficient to lead to hysteresis. In that case, however, there is no microscopic theory for χ available.

ACKNOWLEDGMENTS

We thank M. Bouzid, E. Clément, X. Jia and V. Vidal for discussions. M.W. thanks the Swiss National Science Foundation for support under Grant No. 200021-165509 and the Simons Collaborative Grant "Cracking the Glass Problem" #454953.

[1] Y. Forterre and O. Pouliquen, Annual Review of Fluid Mechanics **40**, 1 (2008).
[2] P. Schall and M. van Hecke, Annual Review of Fluid Mechanics **42**, 67 (2010).
[3] C. H. Scholz, Nature **391**, 37 (1998).
[4] T. Baumberger and C. Caroli, Advances in Physics **55**, 279 (2006).
[5] G. MiDi, The European Physical Journal E: Soft Matter and Biological Physics **14**, 341 (2004-08-01).
[6] F. da Cruz, S. Emam, M. Prochnow, J.-N. Roux, and

F. m. c. Chevoir, Phys. Rev. E **72**, 021309 (2005).
[7] P. Jop, Y. Forterre, and O. Pouliquen, Nature **441**, 727 (2006).
[8] J. A. Dijksman, G. H. Wortel, L. T. van Dellen, O. Dauchot, and M. van Hecke, Physical review letters **107**, 108303 (2011).
[9] O. Kuwano, R. Ando, and T. Hatano, Geophysical Research Letters **40**, 1295 (2013).
[10] G. Wortel, O. Dauchot, and M. van Hecke, Physical Review Letters **117**, 198002 (2016).
[11] B. Andreotti, Y. Forterre, and O. Pouliquen, *Granular media: between fluid and solid* (Cambridge University Press, 2013).
[12] P. A. Johnson, H. Savage, M. Knuth, J. Gomberg, and C. Marone, Nature **451**, 57 (2008).
[13] H. Lastakowski, J.-C. Géminard, and V. Vidal, Scientific reports **5** (2015).
[14] S. C. du Pont, P. Gondret, B. Perrin, and M. Rabaud, Physical review letters **90**, 044301 (2003).
[15] P.-E. Peyneau and J.-N. Roux, Physical review E **78**, 011307 (2008).
[16] For discontinuous, unphysical dissipation mechanisms hysteresis can occur even without friction [45].
[17] H. J. Melosh, Journal of Geophysical Research: Solid Earth (1978–2012) **84**, 7513 (1979).
[18] H. Melosh, Nature **379**, 15 (1996).
[19] A. Lucas, A. Mangeney, and J. P. Ampuero, Nature communications **5** (2014).
[20] D. Sornette and A. Sornette, Bulletin of the Seismological Society of America **90**, 781 (2000).
[21] E. DeGiuli, G. Düring, E. Lerner, and M. Wyart, Physical Review E **91**, 062206 (2015).
[22] M. Müller and M. Wyart, Annual Review of Condensed Matter Physics **6**, 177 (2015).
[23] J. Lin, E. Lerner, A. Rosso, and M. Wyart, Proceedings of the National Academy of Sciences **111**, 14382 (2014).
[24] M. Wyart, Phys. Rev. Lett. **109**, 125502 (2012).
[25] E. Lerner, G. During, and M. Wyart, Soft Matter **9**, 8252 (2013).
[26] E. Azéma and F. Radjai, Physical review letters **112**, 078001 (2014).
[27] R. C. Hurley and J. E. Andrade, Granular Matter **17**, 287 (2015).
[28] E. DeGiuli, J. McElwaine, and M. Wyart, Phys. Rev. E **94**, 012904 (2016).
[29] P.-E. Peyneau, *Etude du comportement et du compactage de pates granulaires par simulation numerique discrete*, Ph.D. thesis, Ecole des Ponts ParisTech (2009).
[30] E. Lerner, G. Düring, and M. Wyart, Proceedings of the National Academy of Sciences **109**, 4798 (2012).
[31] For highly deformable particles flow occurs via a succession of saddle node bifurcations in the energy landscape called shear transformations. Mechanical noise can then speed up flow by allowing for jumps over barriers of potential energy before these are destroyed by shear. This mechanism can cause hysteresis, see [46] for a recent discussion. In our framework such effects can be accounted for by replacing χ by the relative mechanical energy $\mathcal{R}$ in Eq.2. For nearly hard frictionless particles, there is currently no evidence that this phenomenon is at play [15], presumably because the system flows along floppy modes [30] and no jumps over barriers are needed.
[32] N. Menon and D. J. Durian, Science **275**, 1920 (1997).
[33] P. Olsson, Phys. Rev. E **82**, 031303 (2010).
[34] M. Trulsson, E. DeGiuli, and M. Wyart, Physical Review E **95**, 012605 (2017).
[35] The Q dependence is readily obtained in the Eqs.9,10,11,12 by replacing Δ by Δ/Q^2.
[36] X. Jia, T. Brunet, and J. Laurent, Physical Review E **84**, 020301 (2011).
[37] I. Agnolin and J.-N. Roux, Phys. Rev. E **76**, 061302 (2007).
[38] A. L. Sellerio, D. Mari, G. Gremaud, and G. D'Anna, Physical Review E **83**, 021301 (2011).
[39] M. F. Melhus and I. S. Aranson, Granular matter **14**, 151 (2012).
[40] P. A. Johnson and X. Jia, Nature **437**, 871 (2005).
[41] K. Xia, S. Huang, and C. Marone, Geochemistry, Geophysics, Geosystems **14**, 1012 (2013).
[42] P. Charbonneau, J. Kurchan, G. Parisi, P. Urbani, and F. Zamponi, Nature communications **5** (2014).
[43] G. Di Toro, R. Han, T. Hirose, N. De Paola, S. Nielsen, K. Mizoguchi, F. Ferri, M. Cocco, and T. Shimamoto, Nature **471**, 494 (2011).
[44] B. Metzger and Y. Forterre, (2017).
[45] D. Vågberg, P. Olsson, and S. Teitel, arXiv preprint arXiv:1703.01652 (2017).
[46] K. Karimi, E. E. Ferrero, and J.-L. Barrat, Physical Review E **95**, 013003 (2017).
[47] K. Kamrin and G. Koval, Computational Particle Mechanics **1**, 169 (2014).

VI. SUPPLEMENTARY MATERIAL

System-size dependence of hysteresis magnitude –

As described in the main text, when smaller systems are considered, the magnitude of hysteresis is expected to increase. This can be inferred from Fig.1c in the main text. Defining $\Delta\mu_{hyst} \equiv \mu(I = 2 \times 10^{-5}) - \mu(I_*)$, we show directly the depth of the minimum for all data in Fig. 7. Error bars are determined as follows: splitting the total strain into halves, for each run we compute $\Delta\mu_{hyst}$ in each half of strain. The error bar is the standard deviation of these values.

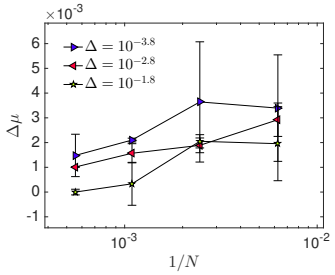

FIG. 7: Hysteresis magnitude as a function of N and Δ.

Phenomenological Model Parameters – The parameters μ_c and c_1 in the phenomenological model can be estimated from existing data [28, 47]. Fig.8a shows μ for a range of μ_p. For realistic μ_p in the range $0.2 < \mu_p < 0.8$, we find $0.23 < \mu < 0.27$. In the main text we take $\mu_c = 0.2$.

We also use the linear form of $\mu(I)$ at intermediate I. Experiments and simulations are often fit to a form $\delta\mu(I) = c_1 I_1/(1 + I_1/I)$, which behaves as $\delta\mu(I) \approx c_1 I$ for I in the dense regime, $I \ll I_1 \approx 0.3$ [1, 47]. Here $c_1 \approx 1.4$ independently of μ_p [47].

Finally, to show the predictions of Eq.2, we use a functional form of $\chi(I, \Delta)$ determined from data. As shown in Fig.8 for $\Delta = 10^{-3.8}$ and various N, our data is very well fit by

$$\chi = \frac{\sqrt{a_1 + a_2 (I/\Delta^{1/4})^{2a_3}}}{1 + a_4 (I/\Delta^{1/4})^{a_3}} \tag{15}$$

The constant a_1 vanishes as $N \to \infty$; we use this large N version in Fig. 1c in the main text.

Finite-size effects in χ – χ has a plateau value as $I \to 0$ that depends on N. Using the fit form described above, we find that all data can be collapsed onto a master curve with finite-size scaling, as shown in Fig. 9a for $\Delta = 10^{-3.8}$. The decay of $\chi_c = \chi(I \to 0)$ with N is shown in Fig.9b.

If the existence of χ_c is taken into account in the theory, this changes Eq.(8) to

$$\chi - \chi_c \propto \frac{1}{2}\mathcal{R}^{\frac{1+\theta_s}{2}}, \tag{16}$$

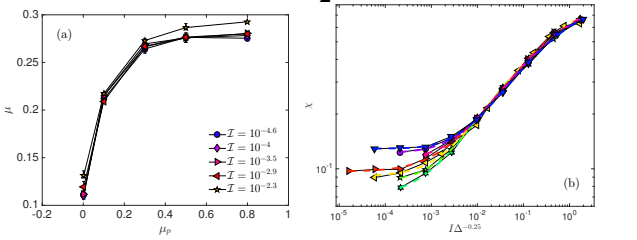

FIG. 8: (a) Dependence of μ_c on the microscopic friction coefficient μ_p. (b) Fits to Eq. 15 for $\Delta = 10^{-3.8}$ and various N (labels in Fig. 9a).

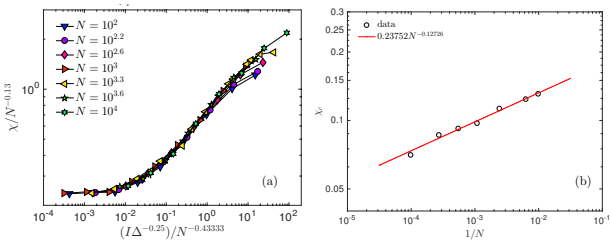

FIG. 9: (a) Finite-size scaling for χ at $\Delta = 10^{-3.8}$. (b) Vanishing of $\chi_c = \chi(I \to 0)$ as $N \to \infty$.

giving

$$\chi^2(\chi - \chi_c)^{\frac{2}{1+\theta_s}} \propto Q\left(\frac{I}{\Delta^{1/4}}\right)^2 \tag{17}$$

Eq. 17 is a closed equation for $\chi(I/\Delta^{1/4})$, and can be solved numerically. As in the main text, we predict that χ depends on $I/\Delta^{1/4}$, as verified in Fig.2. The effect of χ_c in Eq. 17 is to saturate χ at small $I/\Delta^{1/4}$, as shown by the dash-dotted line in Fig.2.